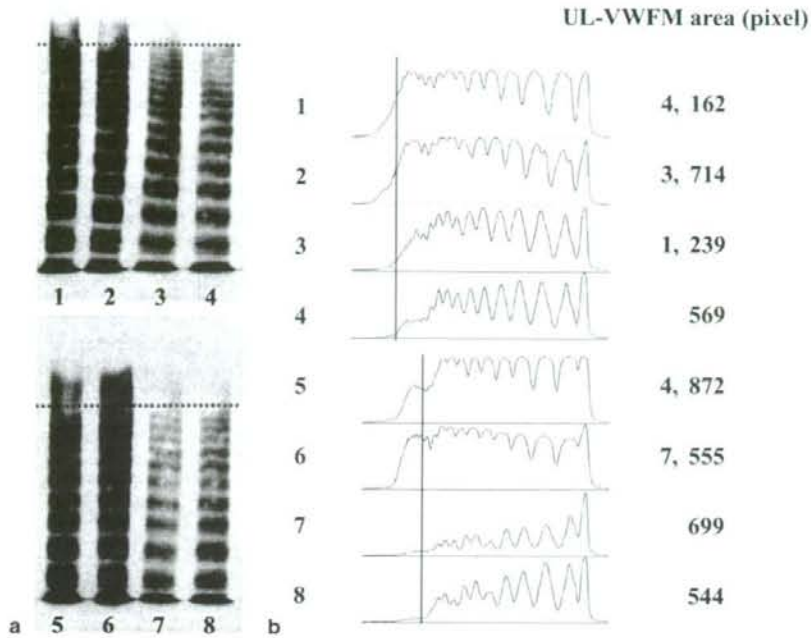

Fig. 3a,b. von Willebrand factor (VWF) multimeric analysis in two representative patients and its densitometric analysis. *1*, patient 1 before PCI in acute phase of AMI; *2*, after PCI of patient 1; *3*, chronic phase of patients 1; *4* and *8*, normal plasma; *5*, before PCI of patient 2; *6*, after PCI of patient 2; *7*, chronic phase of patient 2. **a** von Willebrand factor multimeric analysis was performed using 1% agarose gel electrophoresis. **b** Densitometric analyses of unusually large VWF multimer (*UL-VWFM*) using NIH image J (developed by the National Institute of Health, http://rsb.Info.nih.gov/nih-image/). UL-VWF multimer was detected in samples obtained from the femoral vein before and after PCI in all AMI patients tested, though it was not detected in samples collected during the chronic phase

controls (3.3 ± 1.4), though there was no significant difference in the ratio among sampling points (Fig. 2c). In the chronic phase, those ratios decreased to levels similar to those seen in age-matched controls (FV, 3.2 ± 1.9; Ao, 3.0 ± 1.6; Cs, 3.0 ± 1.5) (Fig. 2c).

Detection of UL-VWFM

We analyzed UL-VWFM in 6 out of 26 AMI patients. UL-VWFM was detected in samples obtained from the FV before and after PCI in all patients (Fig 3a). It was not detected in samples collected during the chronic phase (Fig. 3a). To more easily quantify UL-VWFM levels, we performed densitometric analysis (Fig. 3b).

Circadian variation in plasma VWF:Ag and ADAMTS13 activity

Von Willebrand factor antigen was significantly higher in the morning (100% ± 42%) than in the evening (89% ± 41%) (Fig. 4a); however, for ADAMTS13 activity there was no significant difference between the morning (55% ± 13%) and the evening (61% ± 18%) (Fig. 4b). The ratio of VWF:Ag to ADAMTS13 activity was significantly higher at 09:30 (1.9 ± 0.8) than at 20:00 (1.5 ± 0.8) ($P < 0.05$, Fig. 4c).

Discussion

In the present study we simultaneously measured the activity of ADAMTS13 and the levels of its substrates (VWF:Ag and UL-VWFM) in plasma samples obtained from the FV, Ao, and Cs during the acute and chronic phases of AMI. We demonstrate for the first time that during the acute phase, the ratio of VWF:Ag to ADAMTS13 activity in AMI patients was significantly higher at all three sampling sites than in the peripheral blood of age-matched controls and that during the chronic phase of AMI, these ratios had returned to levels similar to those seen in age-matched controls. Moreover, UL-VWFM was detected during the acute phase but not in the chronic phase of AMI, in agreement with recent reports by Sakai et al.[6] and Goto et al.[12] In agreement with our findings, Kaikita et al.[13] also reported that the ratio of VWF:Ag to ADAMTS13 activity in peripheral venous plasma is higher in AMI patients than in those with stable exertional angina and chest pain syndrome.

During the last decade, evidence has accumulated that release of VWF:Ag from endothelial cells and platelets is a key early step toward occlusive thrombus formation in the coronary circulation. With that in mind, before the beginning of the present study we hypothesized that VWF:Ag would be much higher in the Cs than in the Ao or FV, and that ADAMTS13 activity might be lower in the Cs than in the FV or Ao. However, our study showed that there was

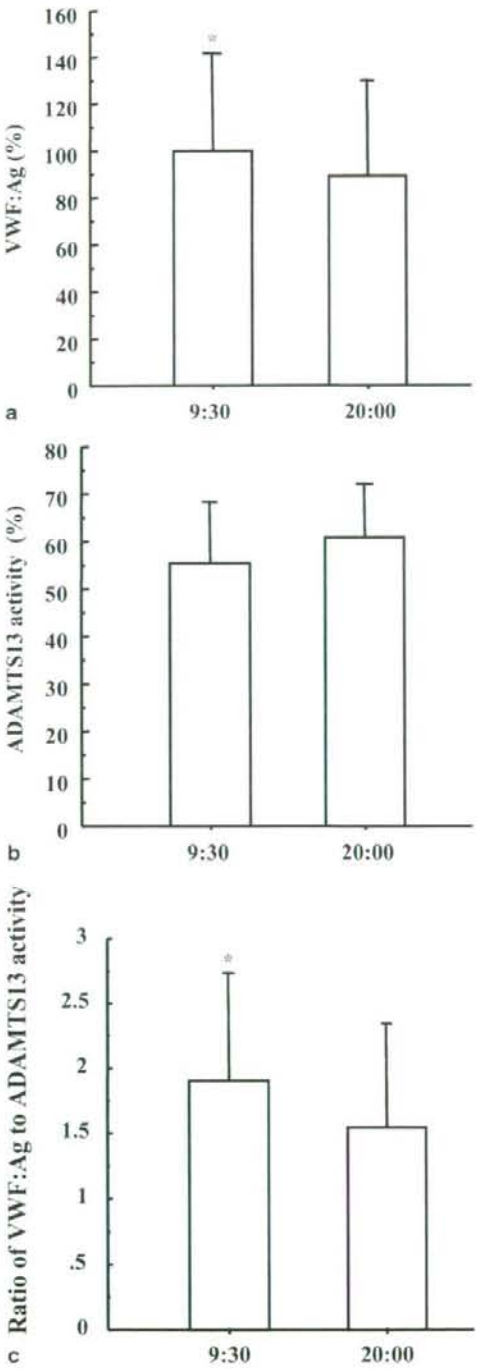

Fig. 4a–c. Comparison with von Willebrand factor antigen (*VWF:Ag*), ADAMTS13, and the ratio of VWF:Ag to ADAMTS13 activity between in the morning and in the evening. **a** VWF:Ag was significantly higher in the morning (100% ± 42%) than in the evening (89% ± 41%). **b** ADAMTS13 activity was no significant difference between in the morning (55% ± 13%) and the evening (61% ± 18%). **c** The ratio of VWF:Ag to ADAMTS13 activity was significantly higher at 09:30 than at 20:00. Shown are mean ± SD. $^{*}P < 0.05$ vs 20:00

no significant difference in the plasma level of VWF:Ag, ADAMTS activity, and the ratio of VWF:Ag to ADAMTS13 activity among three sampling points, clearly indicating that AMI is not a local but rather a systemic prothrombotic condition. In other words, the present findings support the recent concept that occlusive coronary thrombi develop in vulnerable blood (prone to thrombosis) or in vulnerable patients.[14,15] Further studies are necessary to clarify whether increased VWF may lead to the formation of coronary thrombi or whether coronary thrombi itself may cause elevation of VWF levels in AMI.

It was previously reported that AMI frequently occurs in the morning, between 06:00 and 12:00, a vulnerable period for cardiovascular events,[16] and also frequently occurs after physical exercise, especially in the sun during summer. In that regard, we observed that the ratio of VWF:Ag to ADAMTS13 activity was higher in the morning than in the evening. Acute myocardial infarction is also more frequently observed in aged men than in young men. We previously reported that plasma ADAMTS13 activity declines and plasma VWF:Ag levels increase with increasing age, and that detectable levels of UL-VWFM were circulating in some older people.[11] Here, we confirmed that plasma VWF:Ag is 50% higher while plasma ADAMTS13 activity is nearly 50% lower in healthy age-matched control subjects as compared to young healthy subjects, resulting in a three-fold higher ratio of VWF:Ag to ADAMTS13 activity in the former than in the latter. Interestingly, we have also observed that physical exercise increases the ratio of VWF:Ag to ADAMTS13 activity in healthy men.[17] Thus the simultaneous measurement of ADAMTS13 activity and its substrate, VWF:Ag level, is useful in understanding the pathology of thrombotic diseases.

Although it is not possible to identify the precise site of production of VWF and ADAMTS13, our findings (together with those of others[5,6]) suggest that, during the acute phase of AMI, production of VWF is increased not only in coronary arterial endothelial cells and/or locally activated platelets, but also in systemic vascular beds and/or circulating endothelial cells. ADAMTS13 is mainly produced in hepatic stellate cells,[18] and is also synthesized in both human endothelial cells[19] and platelets,[20] suggesting that this enzyme is produced in the systemic circulation as well as in the liver.

In summary, we observed increased plasma VWF:Ag levels and relatively decreased ADAMTS13 activity in both systemic and coronary circulation during the acute phase of AMI, suggesting that an imbalance between the enzyme and its substrate may play an important predictive role in the formation of occlusive thrombi in a coronary

artery, ultimately leading to AMI. Further analysis of the production–consumption relation between VWF and ADAMTS13 in the coronary and systemic circulations will be necessary to understand the pathophysiological significance of VWF and ADAMTS13 in the formation of occlusive thrombi.

Acknowledgments This work was supported in part by research grants from the Ministry of Education, Culture, Sports, Science and Technology (to S.U., M.M., M.U., and Y.S.) and the Ministry of Health, Labour and Welfare (to M.M., Y.F., and Y.S.) of Japan.

References

1. Hoshiba Y, Hatakeyama K, Tanabe T, Goto S (2006) Co-localization of von Willebrand factor with platelet thrombi, tissue factor and platelets with fibrin, and consistent presence of inflammatory cells in coronary thrombi obtained by an aspiration device from patients with acute myocardial infarction. J Thromb Haemost 4:114–120
2. Mandelkorn JB, Wolf NM, Singh S, Shechter JA, Kersh RI, Rodgers DM, Workman MB, Bentivoglio LG, LaPorte SM, Meister SG (1983) Intracoronary thrombus in nontransmural myocardial infarction and in unstable angina pectoris. Am J Cardiol 52:1–6
3. Murasaki K, Kawana M, Murasaki S, Tsurumi Y, Tanoue K, Hagiwara N, Kasanuki H (2007) High P-selectin expression and low CD36 occupancy on circulating platelets are strong predictors of restenosis after coronary stenting in patients with coronary artery disease. Heart Vessels 22:229–236
4. Ruggeri ZM (1997) von Willebrand factor. J Clin Invest 100: S41–S46
5. Eto K, Isshiki T, Yamamoto H, Takeshita S, Ochiai M, Yokoyama N, Yoshimoto R, Ikeda Y, Sato T (1999) AJvW-2, an anti-vWF monoclonal antibody, inhibits enhanced platelet aggregation induced by high shear stress in platelet-rich plasma from patients with acute coronary syndrome. Arterioscler Thromb Vasc Biol 19:877–882
6. Sakai H, Goto S, Kim JY, Aoki N, Abe S, Ichikawa N, Yoshida M, Nagaoka Y, Handa S (2000) Plasma concentration of von Willebrand factor in acute myocardial infarction. Thromb Haemost 84:204–209
7. Jansson JH, Nilsson TK, Johnson O (1991) von Willebrand factor in plasma: a novel risk factor for recurrent myocardial infarction and death. Br Heart J 66:351–355
8. Folsom AR, Wu KK, Rosamond WD, Sharrett AR, Chambless LE (1997) Prospective study of hemostatic factors and incidence of coronary heart disease. Circulation 96:1102–1108
9. Fujimura Y, Matsumoto M, Yagi H, Yoshioka A, Matsui T, Titani K (2002) von Willebrand factor-cleaving protease and Upshaw-Schulman syndrome. Int J Hematol 75:25–34
10. Kato S, Matsumoto M, Matsuyama T, Isonishi A, Hiura H, Fujimura Y (2006) Novel monoclonal antibody-based enzyme immunoassay for determining plasma levels of ADAMTS13 activity. Transfusion 46:1444–1452
11. Matsumoto M, Kawaguchi S, Ishizashi H, Yagi H, Iida J, Sakaki T, Fujimura Y (2005) Platelets treated with ticlopidine are less reactive to unusually large von Willebrand factor multimers than are those treated with aspirin under high shear stress. Pathophysiol Haemost Thromb 34:35–40
12. Goto S, Sakai H, Goto M, Ono M, Ikeda Y, Handa S, Ruggeri ZM (1999) Enhanced shear-induced platelet aggregation in acute myocardial infarction. Circulation 99:608–613
13. Kaikita K, Soejima K, Matsukawa M, Nakagaki T, Ogawa H (2006) Reduced von Willebrand factor-cleaving protease (ADAMTS13) activity in acute myocardial infarction. J Thromb Haemost 4: 2490–2493
14. Naghavi M, Libby P, Falk E, Casscells SW, Litovsky S, Rumberger J, Badimon JJ, Stefanadis C, Moreno P, Pasterkamp G, Fayad Z, Stone PH, Waxman S, Raggi P, Madjid M, Zarrabi A, Burke A, Yuan C, Fitzgerald PJ, Siscovick DS, de Korte CL, Aikawa M, Airaksinen KE, Assmann G, Becker CR, Chesebro JH, Farb A, Galis ZS, Jackson C, Jang IK, Koenig W, Lodder RA, March K, Demirovic J, Navab M, Priori SG, Rekhter MD, Bahr R, Grundy SM, Mehran R, Colombo A, Boerwinkle E, Ballantyne C, Insull W Jr, Schwartz RS, Vogel R, Serruys PW, Hansson GK, Faxon DP, Kaul S, Drexler H, Greenland P, Muller JE, Virmani R, Ridker PM, Zipes DP, Shah PK, Willerson JT (2003) From vulnerable plaque to vulnerable patient: a call for new definitions and risk assessment strategies: Part II. Circulation 108:1772–1778
15. Goto S (2004) Propagation of arterial thrombi: local and remote contributory factors. Arterioscler Thromb Vasc Biol 24:2207–2208
16. Muller JE, Stone PH, Turi ZG, Rutherford JD, Czeisler CA, Parker C, Poole WK, Passamani E, Roberts R, Robertson T (1985) Circadian variation in the frequency of onset of acute myocardial infarction. N Engl J Med 313:1315–1322
17. Claus RA, Bockmeyer CL, Sossdorf M, Losche W, Hilberg T (2006) Physical stress as a model to study variations in ADAMTS-13 activity, von Willebrand factor level and platelet activation. J Thromb Haemost 4:902–905
18. Uemura M, Tatsumi K, Matsumoto M, Fujimoto M, Matsuyama T, Ishikawa M, Iwamoto T, Mori T, Wanaka A, Fukui H, Fujimura Y (2005) Localization of ADAMTS13 to the stellate cells of human liver. Blood 106:922–924
19. Turner N, Nolasco L, Tao Z, Dong JF, Moake J (2006) Human endothelial cells synthesize and release ADAMTS-13. J Thromb Haemost 4:1396–1404
20. Suzuki M, Murata M, Matsubara Y, Uchida T, Ishihara H, Shibano T, Ashida S, Soejima K, Okada Y, Ikeda Y (2004) Detection of von Willebrand factor-cleaving protease (ADAMTS13) in human platelets. Biochem Biophys Res Commun 313:212–216

Circ J 2004; **68:** 677–682

Identification of Autoantibodies With the Corresponding Antigen for Repetitive Coxsackievirus Infection-Induced Cardiomyopathy

Satoko Takata, MD; Hiroshi Nakamura, MD; Seiji Umemoto, MD; Kazuhito Yamaguchil, DVM*; Taichi Sekine, MSc**; Tomohiro Kato, MD**; Kusuki Nishioka, MD**; Masunori Matsuzaki, MD

Background The hypothesis that viral myocarditis causes an autoimmune response and subsequent dilated cardiomyopathy is controversial. To further investigate the autoimmune mechanism of cardiac dilatation and dysfunction after repeated episodes of viral myocarditis, the cardiac autoantigens induced by repetitive coxsackievirus B3 (CVB3) infection were examined.

Methods and Results Male inbred A/J mice were inoculated intraperitoneally with CVB3 at 3 and 40 weeks of age. At 8 weeks after the second inoculation, the mortality of the repetitive CVB3 group was significantly increased compared with that of the control group, and was associated with a significant reduction in fractional shortening and marked left ventricular dilatation without inflammatory cell infiltration. The cardiac antigens in the repetitive CVB3 infection were identified by 2-dimensional electrophoresis and subsequent liquid chromatography/tandem mass spectrometry (LC-MS/MS) using the serum at 2 weeks after the second inoculation. LC-MS/MS and immunohistochemistry demonstrated α-cardiac actin and heat shock protein 60 (HSP60) as cardiac near-surface antigens induced by the repetitive CVB3 infection. Immunoelectron microscopy disclosed the selective localization of anti-IgM antibody on the membrane of the myocytes in the repetitive CVB3 group.

Conclusions IgM antibodies against α-cardiac actin and HSP60, which were induced by repetitive CVB3 infection, may play an important role in the pathophysiology of the subsequent cardiac dysfunction and dilatation. (*Circ J* 2004; **68:** 677–682)

Key Words: Autoantigen; Autoimmunity; Coxsackievirus; HSP60; Viral Myocarditis

Dilated cardiomyopathy (DCM) is characterized by the dilatation and impaired contraction of the ventricles and clinically progressive heart failure[1] It may be idiopathic, familial/genetic, viral and/or immune, alcoholic/toxic, or associated with recognized cardiovascular disease in which the degree of myocardial dysfunction is not explained by the abnormal loading conditions or the extent of ischemic damage. Although the relationship between viral myocarditis and DCM remains controversial, a causal link has become more evident because of the tremendous developments in the molecular analyses of autopsy and endomyocardial biopsy specimens, new techniques of viral gene amplification, and advances in modern immunology[2,3]

It has already been reported that an autoimmune response plays a key role in the progression after viral myocarditis[3,4] This occurs in the context of a polyclonal stimulation of the immune system after the initial viral assault that may have been already cleared when the autoreactive B- and T-cell response occurs[5] Recently, we demonstrated that repetitive coxsackievirus B3 (CVB3) infection produced cardiac dilatation without inflammatory cell infiltration in the heart of mice with post-myocarditis, and autoimmunity mediated by the circulation of certain antibodies (eg, antibodies against the CVB3 genome or a CVB3-related protein) may be part of the pathogenic mechanism for this phenomenon. Moreover, only the autoreactive IgM antibody was apparent on the cell membrane of the myocytes and interstitial tissue in the repetitive infected mice, and may play a pivotal role in the early response to the virus in our repetitive viral myocarditic mice[6] To identify the autoantigen against the components of the myocardium in repetitive CVB3 myocarditic mice, particularly targeting the cell membrane, we examined whether IgM type-autoantibodies were present in the serum of these animals.

Methods

The experimental protocols used in this study were approved by the Ethics Committee for Animal Experimentation at Yamaguchi University School of Medicine, and carried out according to the Guidelines for Animal Experimentation at Yamaguchi University School of Medicine, and Law No. 105 and Notification No. 6 of the Japanese Government.

(Received November 28, 2003; revised manuscript received April 27, 2004; accepted April 30, 2004)

*Department of Cardiovascular Medicine and *Institute of Laboratory Animals, Yamaguchi University Graduate School of Medicine, Ube, and **Division of Rheumatology, Immunology and Genetics Program, Institute of Medical Science, St Marianna University School of Medicine, Kawasaki, Japan*

Mailing address: Masunori Matsuzaki, MD, PhD, Department of Cardiovascular Medicine, Yamaguchi University Graduate School of Medicine, 1-1-1 Minami Kogushi, Ube, Yamaguchi 755-8505, Japan. E-mail: ninai@yamaguchi-u.ac.jp

Experimental Protocol

Three-week old, inbred, certified, virus-free A/J (H-2a) male mice were purchased from Japan SLC (Shizuoka, Japan). Fourteen normal mice were also housed for 40 weeks as a control (3W–/40W–). The CVB3 (Nancy strain) was obtained from the American Type Culture Collection and stored at –80°C until use. Each 3-week old mouse was initially infected by an intraperitoneal injection of 2×10^4 plaque-forming units of CVB3 in 0.2 ml of saline. The infected mice were isolated, 5 per cage, in a special unit for 37 weeks (3W+/40W–). A total of 31 mice first inoculated at 3 weeks were reinfected in the same manner with CVB3 at 40 weeks (3W+/40W+). In addition, 5 normal mice were inoculated at 40 weeks (3W–/40W+) as a further control group. At 8 weeks after reinfection, the mice were weighed and killed with KCl injection via the inferior vena cava to stop the heart in end-diastole. Body weight was measured, and the hearts, lungs, and livers were excised and weighed. The control mice were treated in the same manner, but with saline that did not contain the virus.

Morphometry and Histopathological Study

The ventricles from the mice killed at 8 weeks after the second inoculation were halved transversely and one portion was fixed with 10% formalin solution, then embedded in paraffin solution and sectioned into slices of 4-mm thickness stained with hematoxylin-eosin and Azan solutions. The left ventricular (LV) dimensions and wall thickness were measured using the transverse section of the middle portion of the ventricle. The cavity dimensions and wall thickness of the left ventricle were calculated according to the method of Matsumori et al[7] Cardiac fibrosis was also evaluated quantitatively using a Fotovision FV-10 camera (Fuji Film Co, Japan) and a (Macintosh 8500/120) computer equipped with NIH Image version 1.62 software.

Echocardiography

Prior to death at 8 weeks after the second inoculation, the mice underwent light anesthesia with ether. The LV end-diastolic dimension (EDD), end-systolic dimension (ESD), and fractional shortening (%FS) were obtained by averaging the data from 3 cardiac cycles using an echocardiographic system (ALOKA 5500; Aloka, Japan) with a dynamically focused 10-MHz linear array transducer.

Immunoelectron Microscopy

Immunoelectron microscopy was performed by the method of Yamaguchi et al[8] Briefly, the hearts at 2 weeks after the second inoculation were fixed by perfusing with paraformaldehyde. For immunostaining, horseradish peroxidase (HRP) conjugated anti-mouse IgM was used. Sections 10–19 nm thick were examined with a JEOL 200 CX transmission electron microscope at 160 kV. Sarcomere lengths were measured in a blinded fashion at a magnification of 3,700. This process was repeated for 50 fields per animal.

Two-Dimensional Western Blotting

Fresh murine heart tissue at 2 weeks after the second inoculation was minced and resuspended in 5 volumes of STE buffer containing 320 mmol/L sucrose, 10 mmol/L Tris–HCl, pH 7.4, 1 mmol/L EGTA, 5 mmol/L NaN3, 10 mmol/L -mercaptoethanol, 20 mmol/L leupeptin, 0.15 mmol/L pepstatin A, 0.2 mmol/L phenylmethylsulfonyl fluoride, and 50 mmol/L NaF, with a Polytron homogenizer (PT1200; Kinematica, Germany), at its maximum speed for 30 s, repeated 3 times. Homogenates were mixed with an equal volume of STE buffer and centrifuged at 1,000 G for 10 min, and the supernatant was centrifuged at 100,000 G for 60 min. The 1,000-G and 100,000-G pellets were designated as P1 and P2 fractions, respectively, and the 100,000-G supernatant as the S fraction. The P1 and P2 fractions were resuspended in STE buffer. The total protein concentration in each fraction was determined, using bovine serum albumin as a standard[9]

The extracted protein samples were diluted in a rehydration buffer (8 mol/L urea, 2% CHAPS, 2.8 mg/ml dithiothreitol (DTT), trace of bromphenol blue) containing 0.5% immobilized pH gradient (IPG) buffer (pH range 3–10; Amersham Pharmacia Biotech, Sweden), and loaded onto 7 cm Immobiline Drystrips (Amersham Pharmacia Biotech) in the IPG reswelling tray (Amersham Pharmacia Biotech) at room temperature overnight. Up to 400 mg of the extracted proteins was applied onto the drystrip gels for western blotting, and up to 1,000 mg for the analysis by mass spectrometry. Isoelectric focusing (IEF) was performed in a horizontal electrofocusing apparatus (MultiPhor II; Pharmacia Biotech, Sweden) according to the manufacturer's instructions. After the IEF, the IPG strips were equilibrated in 2 equilibration solutions. The first equilibration solution consisted of 10 mg DTT per 1 ml sodium dodecyl sulfate (SDS) equilibration buffer (1.5 mol/L Tris-Cl, pH8.8; 6 mol/L urea, 30% glycerol, 2% SDS), and the second equilibration solution consisted of 25 mg iodoacetamide per 1 ml SDS equilibration buffer. The equilibrated strips were placed on top of a 12.5% SDS polyacrylamide gel electrophoresis (PAGE) slab and sealed with 0.5% lower melt gel, and then the second electrophoresis was performed with a 40 mA constant current in the separating gel at 20°C.

After electrophoresis, the SDS-PAGE gels were stained with Coomassie Brilliant Blue (CBB) or used for protein transfer onto nitrocellulose membranes (Protran, Schleicher & Schuell, Germany). In the western blotting, the membranes were blocked in phosphate-buffered saline (PBS) containing 1% bovine serum albumin (BSA) and 0.1% Tween 20 for 1 h, washed in PBS with 0.1% Tween 20 (PBST) for 30 min, and incubated with serum samples, which were collected from mice at 2 weeks after the second inoculation, diluted adequately in PBST containing 1% BSA for 1 h. After 5 washings in PBST, the bound antibodies were reacted with HRP-conjugated goat anti-mouse IgM (Sigma, St Louis, MO, USA) for 1 h. Finally, the bound antibodies were visualized by diaminobenzidine.

Mass Determination and Mass Fingerprinting

Liquid chromatography/tandem mass spectrometry (LC-MS/MS) was performed as follows to determine the molecular weight of the protein spots. Protein spots on the gel stained with CBB, which corresponded to the positive spots on the western blotting membranes, were recovered and then the recovered gel fragments were washed in double distilled water for 15 min, de-colored in 50 ml decoloring solution (0.1 mol/L ammonium hydrogen carbonate, 50% methanol) at 40°C for 15 min, and cut into small pieces. The gel pieces were re-hydrated in 20 ml trypsin solution (0.1 pmol/ml trypsin in 50 mmol/L Tris-HCl; Wako Pure Chemical Industries, Ltd, Japan) and incubated at 37°C. The digested peptides were extracted from the gel pieces using trifluoroacetic acid (TFA) and acetonitrile.

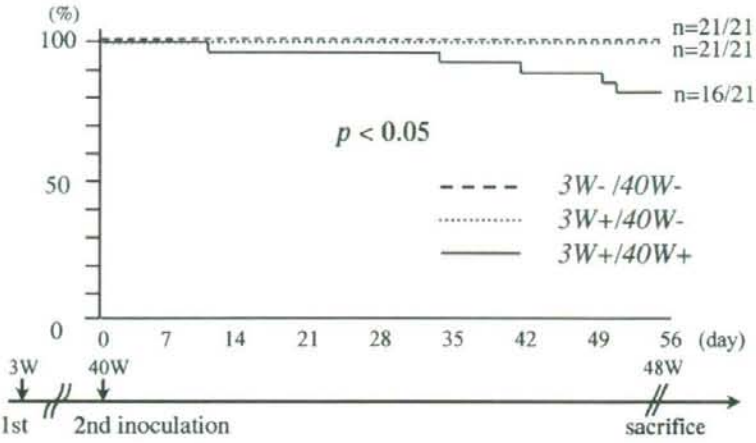

Fig 1. Survival curve after the second inoculation in viral myocarditic mice at 40 weeks. A survival reduction of 23.8% was observed in the repetitive group (3W+/40W+) compared with the control group (3W−/40W−) at 8 weeks after the second inoculation. *p<0.05 vs both the 3W−/40W− and 3W+/40W− groups. No mice died after the second vehicle injection.

Specifically, the digested products were added to 50 ml of 0.1% TFA/50% acetonitrile, vortexed, and sonicated for 10 min. After centrifugation, the supernatant was recovered. After 2 more cycles of this extraction, a similar extraction was performed with 50 ml of 0.1% TFA/80% acetonitrile. The collected supernatant was centrifuged again, filtered, and concentrated down to 50 ml in an evaporator, and was then desalted using a Zip-Tip desalting column (Millipore Corp, Milford, MA, USA). The peptide sample solution was stored at −20°C until mass spectrometry analysis.

The mass of the digested peptides in the samples was determined using a mass spectrometer with matrix-assisted laser desorption/ionization-time of flight (MALDI-TOF; Voyager DE-STR; PerSeptive Biosystems, USA). Alpha-cyano-4-hydroxycinnamic acid was used as an assisting matrix. A list of the determined peptide masses was made by a mass fingerprint search of the NCBI protein databases using the Mascot software program (Matrix Science, Ltd, UK), in which the NCBI protein databases were searched.

Immunohistochemistry

For immunoenzymatic staining, the remaining ventricular portion was quickly frozen with OCT compound (Miles, Inc, USA) in liquid nitrogen and stored at −80°C. The frozen specimens were sectioned at 4-mm thickness. Immunoenzymatic staining was performed with a DAKO LSAB kit (DAKO, USA) according to the manufacturer's instructions. Antibody against murine heart shock protein 60 (HSP60) (Stressgen, Canada) was used as the primary antibody.

Statistical Analysis

Data were expressed as the mean ± SD. Statistical analysis of the data was performed by an analysis of variance with multiple comparisons. The survival of all animals was assessed by Kaplan-Meier analysis. A level of $p<0.05$ was considered statistically significant.

Results

Survival Rates

Fig 1 shows the survival curve at 8 weeks after the second inoculation at 40 weeks. Five of the 21 mice died after the second CVB3 inoculation (mortality rate: 23.8%, $p<0.05$). All of the dead mice had pleural effusion and ascites, indicating that they probably died from heart failure. No mice died after the second vehicle injection.

Table 1 Assessment of the Systemic Parameters of Viral Myocarditis

	Group		
	3W−/40W−	*3W+/40W−*	*3W+/40W+*
Physiological analysis			
No. of experiments	*5*	*5*	*5*
Body weight (g)	*29.2±2.8*	*30.2±2.5*	*26.3±2.0†*
Heart weight (mg)	*108±4.2*	*140.8±38.4*	*201.4±91.0**
Lung weight (mg)	*212±3.6*	*199±92*	*221±93*
Liver weight (mg)	*1,173±268*	*1,023±101*	*967±4*
HW/BW(mg/g)	*3.73±0.45*	*4.65±1.11*	*7.89±4.15**
LW/BW (mg/g)	*7.25±0.90*	*6.55±2.75*	*8.5±4.38*
LIW/BW (mg/g)	*40.21±8.31*	*34.21±2.44*	*36.28±1.99*
Morphometry			
Wall thickness (mm)	*0.8±0.1*	*0.7±0.1*	*0.7±0.1*
Fibrosis (%)	*3.1±0.7*	*16.5±11.1**	*26.9±6.0*†*
Inflammatory grading	*0*	*0.2±0.4*	*0.2±0.4*
Echocardiography			
LVEDD (mm)	*2.4±0.3*	*2.6±0.4*	*3.4±0.3*†*
LVESD (mm)	*0.9±0.1*	*1.3±0.3**	*2.4±0.5*†*
%FS (%)	*60.8±5.4*	*50.6±7.6**	*29.6±7.9**

HW/BW, ratio of heart weight/body weight; LW/BW, ratio of lung weight/body weight; LIW/BW, ratio of liver weight/body weight; LVEDD, left ventricular end-diastolic dimension; LVESD, left ventricular end-systolic dimension; %FS, fractional shortening.
*Values are the mean ± SD. *p<0.05 vs the 3W−/40W− group. †p<0.05 vs the 3W+/40W− group.*

Physiological Analysis

The mean body weight in the 3W+/40W+ group was significantly reduced compared with that in the 3W+/40W− group ($p<0.05$). The heart weight and the ratio of heart weight/body weight in the 3W+/40W+ group was significantly increased compared with that in the 3W−/40W− group ($p<0.05$) (Table 1). There were no differences between the 3W−/40W− and 3W+/40W− groups in body weight or heart weight, or in the ratio of the heart weight/body weight. In addition, there were no significant differences in the weights of the lungs and livers among the 3 groups.

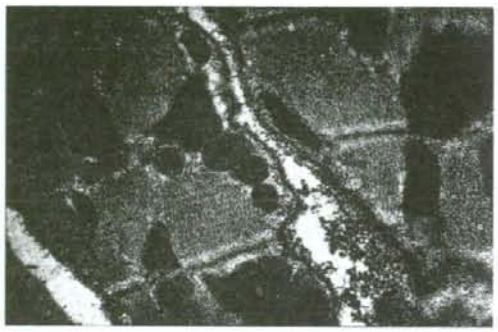

Fig 2. Ultrastructural localization of anti-heart antibodies was confirmed on the surface of the myocytes and interstitial tissue with immunoelectron microscopy (×10,000).

Histology

There was a significant increase in the LV dimension in the 3W+/40W+ group compared with the 3W+/40W– group ($p<0.05$). The ratio of cardiac fibrosis in the 3W+/40W– and 3W+/40W+ groups was significantly higher than in the 3W–/40W– group ($p<0.05$). The ratio of cardiac fibrosis in the 3W+/40W+ group was the highest among the 3 groups (Table 1). There was no significant difference in the mean wall thickness among the 3 groups. Inflammatory cell infiltration was less than 5% in all groups (Table 1).

Echocardiography

To evaluate cardiac function, we performed transthoracic echocardiography at 8 weeks after the second inoculation. Both the LVEDD and LVESD of the 3W+/40W+ group were significantly increased compared with those of the other 2 groups; %FS was significantly reduced in the 3W+/40W+ group compared with that in the other 2 groups (Table 1).

Immunoelectron Microscopy

The sarcomere length in the 3W+/40W+ group was 1.8±0.24 mm, which is comparable to the data previously obtained.[6] Staining of bound IgM in the myocardium was recognized only in the 3W+/40W+ group. The cell membranes of the myocytes and interstitial tissue were positively stained with the anti-IgM antibody by immunoelectron microscopy (Fig 2).

Two-Dimensional Western Blotting and Subsequent LC-MS/MS

On 2-dimensional western blotting, 2 spots were detected as A3 (pI 5.2) and A5 (pI 5.9) in the membranous fraction that specifically cross-reacted with the serum in the 3W+/40W+ group (Fig 3). By subsequent LC-MS/MS, A3 (MW 42001 Da) and A5 (MW 60941 Da) were recognized as a-cardiac actin and HSP60, respectively (Fig 3).

Immunohistochemistry

Because α-cardiac actin is known to be ubiquitously distributed in myocytes, and only HSP60 is reported to be upregulated on the cell surface, as well as in the cytosol and mitochondria in response to many different stresses,[10] we performed further immunohistochemical analysis for HSP60 at 2 weeks after the second inoculation. We showed that HSP60 was positively stained in the myocytes and interstitial tissue (yielding a brown color with a pale blue background) taken from the hearts in the 3W+/40W+ group (Fig 4A). No myocytes were positively stained with the HSP60 antibody in the 3W–/40W–, 3W+/40W– or 3W–/40W+ groups (Fig 4B,C and 4, respectively).

Discussion

There is some clinical evidence that DCM is a late sequel of acute or chronic viral myocarditis.[5] Infectious and autoimmune myocarditis has also been extensively proven using murine and rat models.[3–5] We previously demonstrated that repetitive CVB3 infection in mice could cause LV dilatation with dysfunction through autoantibodies,

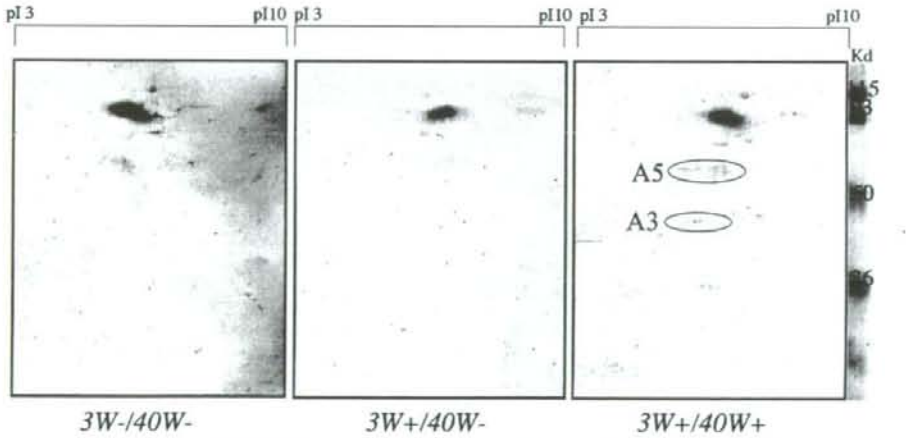

Fig 3. Two-dimensional western blotting with the serum in the 3W–/40W–, 3W+/40W–, and 3W+/40W+ groups. Two spots were detected as A3 and A5 in the membranous fraction that specifically cross-reacted with the serum in the 3W+/40W+ group compared with the other 2 groups. A3 and A5 were recognized as α-cardiac actin and murine HSP60, respectively, by subsequent LC-MS/MS.

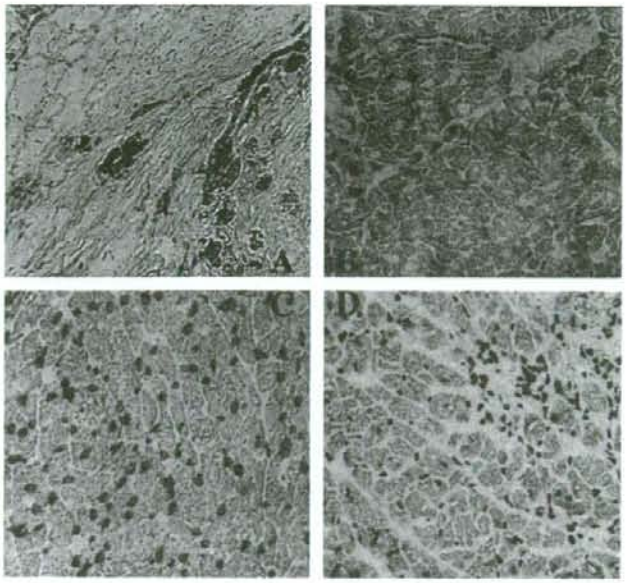

Fig 4. Immunohistochemistry of the myocardium with the anti-HSP60 antibody. The HSP60-positive cells were scattered in the myocardium in the 3W+/40W+ mouse (A). No specific staining for the anti-HSP60 antibody was observed in the heart tissue of either the 3W−/40W− (B), 3W+/40W− (C), or 3W−/40W+ (D) groups.

which were immunologically maximally activated at 2 weeks after the second CVB3 inoculation[6] Moreover, these pathophysiological changes were present even at 8 weeks after the second inoculation. Electron microscopy showed that these antibodies belong to the IgM subtype, and were distributed on the surface of the myocytes and interstitial tissue at 2 weeks after the second viral inoculation in mice. The results of our study are entirely different from the previously reported anti-heart antibodies in viral myocarditis[5] First, in the present study repetitive CVB3 infection produced cardiac dilatation and dysfunction without inflammatory cell infiltration in post-myocarditic mice. This poor T cell response may be related to the protective effect of neutralizing antibody against CVB3 induced by the first inoculation, as well as to CVB3 being less able to cause myocardial lesions related to senescence[6] Second, antibodies that react to the membranous fraction of normal myocytes were produced in the repetitive viral infection, but not in the post-myocarditis mice with simple viral infection. Third, the antibodies were classified as the IgM subtype, as distinct from the other IgG-type antibodies, such as ADP-ATP carrier protein and cardiac sarcoplasmic reticulum calcium ATPase, which were previously identified as cardiac autoantibodies[5] Fourth, the antibodies reacted to the membrane fraction of the myocytes, so that these antibodies identified in the serum of the repetitive myocarditic mice could easily bind the targeting antigen and cause immunological cytotoxicity accompanied by activation of the complementary system in vivo[11] It has also been reported that some anti-heart IgM autoantibodies can activate the complementary system and cause subsequent cardiac damage, especially in membranous proteins such as myolemmal[12] Fifth, we identified 2 autoantibodies (α-cardiac actin and HSP60) against the cardiac membrane protein. Finally, we have already reported that interleukin-1α and tumor necrosis factor-α were elevated in our model[6] They are able to potentiate the immune response and induce cell death, both of which appear to have a special importance in the pathogenesis of myocarditis. As a result, the IgM antibodies, which can activate the complementary system, and cytokines may cooperatively cause the cytotoxic effect on the target myocytes.

In patients with histologically proven myocarditis or familial DCM, autoreactive autoantibodies to components of the myocardium are often present, including intracellular targets such as the ADP/ATP translocator and other mitochondrial proteins[13] Dorffel et al demonstrated that the extraction of autoimmunoreactive antibodies by immunoadsorption results in a functional improvement in hemodynamics in DCM patients[14] Those authors have proven indirectly that autoantibodies against the ADP-ATP carrier[15] contractile proteins of cardiomyocytes, and the cardiac β_1-adrenergic receptor[16,17] contribute to cardiac malfunction in DCM. They proposed that the immunoadsorption may be an additional therapeutic possibility for the acute hemodynamic stabilization of patients with severe DCM. Moreover, Kishimoto et al reported that antibody-mediated immune enhancement is involved in the pathogenesis of CBV3 myocarditis in mice[18] Nishimura et al also proved that PD-1, which binds to the 33-kD protein, may be an important factor contributing to autoimmune cardiomyopathy in mice[19] These results raise the possibility that some form of cardiomyopathy may have a CVB3-induced autoimmune basis, and that identifying possible autoantigen(s) may open up new diagnostic and therapeutic approaches for this disease. Regarding their results, molecular mimicry may be involved in these mechanisms[20] This occurs when an immune response mounted by the host against a specific determinant of an infecting viral or bacterial agent cross-reacts with a similar 'mimicked' host sequence, leading to autoimmunity, and, in some cases, tissue injury and disease. However, one question that has been raised is how these antibodies recognize cytosolic antigen in intact myocytes, because these antigens are isolated and tolerated from circulating antibodies[11] Interestingly, Maish et al demonstrated that anti-membrane antibodies circulated not only in

the peripheral blood, but were also bound to the sarcolemma and interstitial tissue in the endomyocardial biopsy specimens of patients[5] Their results are compatible with our electron microscopy findings, indicating that the antibodies belong to the IgM subtype, and respond to the surface of the myocytes in repetitive CVB3 infection. In this study, we compared the serum of repetitive CVB3 with other groups to identify autoantigens in the myocardium, and identified 2 cardiac antigens in the membranous fraction: α-cardiac actin and HSP60. Although α-cardiac actin is a well-known cytosolic component of myocytes, there is a technical limitation to purifying the membrane fraction in the process of extraction from a heart sample[9] As we observed in our study, α-cardiac actin has already been reported as a cytosolic autoantigen in CVB3 myocarditis[21]

In this study, we demonstrated that HSP60 may be a candidate for a membrane-bound autoantigen in repetitive CVB3 inoculation. The HSP family has been identified as a prominent target of ongoing immune responses during microbial infections. Cross-reactive immune responses between mammalian and microbial HSPs have been suggested as underlying several autoimmune and inflammatory disorders, including chronic arthritis, systemic lupus erythematosus, atherosclerosis, Crohn's disease, and diabetes[22] In addition to constituting an endogenous stress response that protects cells from injury, members of the HSP family are also candidate molecules that potentially signal tissue damage or cellular stress to the immune system, the so-called 'danger theory'. The expression of HSP is upregulated rapidly during several forms of cellular stress, and HSP can be released from damaged tissue[23] Portig et al reported that antibodies against HSP60 were found in the sera of patients with DCM, and may interfere with the functions this stress protein plays in cell physiology (ie, protein transport, protein maturation, and protection of the cell under stress conditions)[24] Latif et al also reported that not only was the anti-heart antibody against HSP60 present in the sera, but HSP60 was upregulated in the myocardium of patients with DCM[10] They confirmed that the cell surface expression of HSP60 after heat stress can be visualized using immunofluorescence. Taken together with our results, these findings suggest that IgM antibodies against α-cardiac actin and HSP60, which were induced by repetitive CVB3 infection, may play an important role in the pathophysiology of the subsequent cardiac dysfunction and dilatation.

Conclusions

In the present study, repetitive CVB3 infection caused cardiac dysfunction and dilatation with an induction of a variety of anti-heart antibodies. Exploring the nature of these autoantibodies found in the sera of our model will provide further immunological and virological insights into the mechanism of subsequent DCM after viral myocarditis.

Acknowledgments

We would like to thank Dr Akira Matsumori (Kyoto University, Kyoto, Japan) for his provision of CVB3. In addition, we would like to thank Rie Ishihara and Kazuko Iwamoto for their excellent technical assistance. This study was supported in part by funds from the Idiopathic Cardiomyopathy Research Group of the Ministry of Health and Welfare of Japan.

References

1. Kriett JM, Kaye MP. The registry of the international society for heart transplantation: Seventh official report, 1990. *J Heart Transplant* 1990; **9:** 323–330.
2. Kawai C. From myocarditis to cardiomyopathy: Mechanisms of inflammation and cell death: Learning from the past for the future. *Circulation* 1999; **99:** 1091–1100.
3. Nakamura H, Yamamura T, Umemoto S, Fukuta S, Shioi T, Matsumori A, et al. Autoimmune response in chronic ongoing myocarditis demonstrated by heterotopic cardiac transplantation in mice. *Circulation* 1996; **94:** 3348–3354.
4. Nakamura H, Kato T, Yamamura T, Yamamoto T, Umemoto S, Sekine T, et al. Characterization of T cell receptor b chains of accumulating T cells in chronic ongoing myocarditis demonstrated by heterotopic cardiac transplantation in mice. *Jpn Circ J* 2001; **65:** 106–110.
5. Maisch B, Ristic AD. Humoral immune response in viral myocarditis. *In*: Cooper LT, editor. Myocarditis: From bench to bedside. New Jersey: Humana Press; 2002; 77–108.
6. Nakamura H, Yamamoto T, Yamamura T, Nakao F, Umemoto S, Shintaku T, et al. Repetitive coxsackievirus infection induces cardiac dilatation in post-myocarditic mice. *Jpn Circ J* 1999; **63:** 794–802.
7. Matsumori A, Kawai C. An experimental model for congestive heart failure after encephalomyocarditis virus myocarditis in mice. *Circulation* 1982; **65:** 1230–1235.
8. Yamaguchi K, Takahashi S, Sasaki K, Tonosaki A. Early expression of intercellular adhesion molecule-1 in the corneal endothelium stimulated by endotoxin: An immuno-scanning electron microscopical study. *Jpn J Ophthalmol* 1996; **40:** 12–17.
9. Kawamura S, Yoshida K, Miura T, Mizukami Y, Matsuzaki M. Ischemic preconditioning translocates PKC-δ and -ε, which mediate functional protection in isolated rat heart. *Am J Physiol* 1998; **275:** 2266–2271.
10. Latif N, Taylor PM, Khan MA, Yacoub MH, Dunn MJ. The expression of heat shock protein 60 in patients with dilated cardiomyopathy. *Basic Res Cardiol* 1999; **94:** 112–119.
11. Wraith DC. Immunological tolerance. *In*: Roitt I, Brostoff J, Male D, editors. Immunology, 5th edn. London: Mosby; 1996; 187–198.
12. Olson TM, Kishimoto Y, Whitby FG, Michels VV. Mutations that alter the surface charge of alpha-tropomyosin are associated with dilated cardiomyopathy. *J Mol Cell Cardiol* 2001; **33:** 723–732.
13. Liu PP, Mason JW. Advances in the understanding of myocarditis. *Circulation* 2001; **104:** 1076–1082.
14. Dorffel WV, Felix SB, Wallukat G, Brehme S, Bestrvater K, Hofmann T, et al. Short-term hemodynamic effects of immunoadsorption in dilated cardiomyopathy. *Circulation* 1997; **95:** 1994–1997.
15. Schulze K, Becker BF, Schauer R, Schultheiss HP. Antibodies to ADP-ATP carrier, an autoantigen in myocarditis and dilated cardiomyopathy, impair cardiac function. *Circulation* 1990; **81:** 959–969.
16. Magnusson Y, Marullo S, Hoyer S, Waagstein F, Andersson B, Vahlne A, et al. Mapping of a functional autoimmune epitope on the β1-adrenergic receptor in patients with idiopathic dilated cardiomyopathy. *J Clin Invest* 1990; **86:** 1658–1663.
17. Baba A, Yoshikawa T, Chino M. Characterization of anti-myocardial autoantibodies in Japanese patients with dilated cardiomyopathy. *Jpn Circ J* 2001; **65:** 867–873.
18. Kishimoto C, Kurokawa M, Ochiai H. Antibody-mediated immune enhancement in coxsackievirus B3 myocarditis. *J Mol Cell Cardiol* 2002; **34:** 1227–1238.
19. Okazaki T, Tanaka Y, Nishio R, Mitsuiye T, Mizoguchi A, Wang J, et al. Autoantibodies against cardiac troponin I are responsible for dilated cardiomyopathy in PD-1-deficient mice. *Nat Med* 2003; **9:** 1477–1483.
20. Richardson P, McKenna W, Bristow M, Maisch B, Mautner B, O'Connell J, et al. Report of the 1995 World Health Organization/International Society and Federation of Cardiology Task Force on the definition and classification of cardiomyopathies. *Circulation* 1996; **93:** 841–842.
21. Maisch B, Bauer E, Cirsi M, Kochsiek K. Cytolytic cross-reactive antibodies directed against the cardiac membrane and viral proteins in coxsackievirus B3 and B4 myocarditis: Characterization and pathogenetic relevance. *Circulation* 1993; **87**(Suppl 4)**:** IV-49–IV-65.
22. Oldstone MB. Molecular mimicry and autoimmune disease. *Cell* 1987; **50:** 819–820.
23. Wallin RP, Lundqvvist A, More SH, von Bonin A, Kiessling R, Ljunggren HG. Heat-shock proteins as activators of the innate immune system. *Trends Immunol* 2002; **23:** 130–135.
24. Portig I, Pankuweit S, Maish B. Antibodies against stress protein in sera of patients with dilated cardiomyopathy. *J Mol Cell Cardiol* 1997; **29:** 2245–2251.

Europace (2008) 10, 379–383
doi:10.1093/europace/eum297

Chronic cardiac resynchronization therapy reverses cardiac remodelling and improves invasive haemodynamics of patients with severe heart failure on optimal medical treatment

Tomohito Inage, Teruhisa Yoshida*, Tatsuro Hiraki, Masatsugu Ohe, Tomohiro Takeuchi, Yasutsugu Nagamoto, Yujiro Fukuda, Takeki Gondo, and Tsutomu Imaizumi

Department of Internal Medicine, Division of Cardio-Vascular Medicine, Kurume University School of Medicine, 67 Asahi-machi, Kurume 830-0011, Japan

Received 18 June 2007; accepted after revision 18 December 2007; online publish-ahead-of-print 28 January 2008

KEYWORDS
Resynchronization;
Haemodynamic effect;
Cardiac catheterization;
Reverse cardiac remodelling

Aims The aim of this study was to assess chronic invasive haemodynamic effects of cardiac resynchronization therapy (CRT) in patients with severe heart failure.

Methods and results Seventeen patients with New York Heart Association (NYHA) class III or IV and QRS duration >120 ms on optimal treatments underwent CRT. Haemodynamic data were obtained by cardiac catheterization before and 1 month after CRT. Clinical parameters and exercise tolerance were also evaluated. Chronic CRT improved haemodynamics significantly; mean pulmonary capillary wedge pressure decreased from 15.9 ± 6.1 to 10.2 ± 5.3 mmHg ($P < 0.05$), systolic pulmonary artery pressure decreased from 36.5 ± 13.2 to 26.7 ± 11.9 mmHg ($P < 0.05$), left ventricular end-diastolic pressure decreased from 15.6 ± 7.2 to 10.5 ± 7.3 mmHg ($P < 0.05$), end-diastolic volume decreased from 358.8 ± 84.6 to 322.9 ± 99.0 mL ($P < 0.05$), end-systolic volume decreased from 264.1 ± 67.6 to 219.2 ± 74.3 mL ($P < 0.05$), left ventricular ejection fraction increased from 25.4 ± 6.2 to 33.1 ± 4.9% ($P < 0.05$), and cardiac index increased from 1.9 ± 0.4 to 2.2 ± 0.5 L/min/m^2 ($P < 0.05$). Chronic CRT significantly improved functional capacity such as NYHA classification, 6 min walk distance, and peak oxygen uptake.

Conclusion Chronic CRT improved not only symptoms and exercise tolerance but also invasive haemodynamics associated with reversed cardiac remodelling.

Introduction

Intraventricular conduction delay commonly occurs in patients with chronic heart failure and produces dyssynchronous ventricular contraction that further impairs cardiac function.[1–3] An overwhelming amount of evidence from prospective randomized controlled trials supports the clinical efficacy and safety of cardiac resynchronization therapy (CRT) in patients with moderate or severe heart failure and ventricular dyssynchrony. CRT has been demonstrated to decrease hospitalization and mortality and to improve symptoms, exercise tolerance, and quality of life.[4–10] CRT also has been demonstrated to improve long-term cardiac function assessed by echocardiography.[11–13] However, it is well known that the echocardiographic assessment of cardiac function may not be so accurate in the presence of segmental wall motion abnormality.[14] Moreover, reports of the chronic effects of CRT on invasive haemodynamics have been few. Accordingly, we assessed the chronic haemodynamic effects of CRT by cardiac catheterization in patients with severe heart failure on optimal medical treatment.

Methods

Patients

The entry criteria included New York Heart Association (NYHA) functional class III or IV heart failure and QRS complex duration >120 ms, despite optimal pharmacological therapy in the stable condition for at least 1 month. The drugs prescribed for them were angiotensin-converting enzyme-inhibitor, angiotensin receptor

* Corresponding author. Tel: +81 942 31 7562; fax: +81 942 33 6509.
E-mail address: teruhisa@med.kurume-u.ac.jp

blocker, diuretics, digitalis, and/or β-blocker (*Table 1*). Patients were excluded from the study if they had any of following: unstable angina, acute myocardial infarction, coronary artery revascularization within 3 months before enrolment, treatment with intravenous inotropic agents, or correctable valvular disease. Patients were admitted to our ward to receive optimal medical treatment. When the condition of patients was stable for at least 1 month and no further improvement was obtained with medical treatments, they underwent CRT. In 17 patients, haemodynamic data were obtained before and 1 month after CRT by cardiac catheterization. The pharmacological therapy was not changed in order to evaluate the effect of CRT. Written informed consent was obtained from all patients. The study protocol was approved by the Ethics Committee of human investigations at our institution.

Catheterization protocol and pacemaker implantation procedure

Haemodynamic data were obtained during cardiac catheterization before and 1 month after CRT. Patients were examined while in a supine, non-sedative state. A thermodilution Swan-Ganz catheter (Edwards Lifesciences T173HF6, Irvine, CA, USA) was inserted via the femoral vein and positioned in the pulmonary artery so that mean pulmonary capillary wedge pressure (PCWP) recordings were obtained upon balloon inflation. Cardiac output was recorded in triplicate or until three recordings within 10% of each other were obtained. Systolic pulmonary artery pressure and mean right atrium pressure were also evaluated. Then a 6F pigtail catheter (SPC-454D, Millar Instruments, Houston, TX, USA) was advanced via femoral artery and placed so that the pigtail tip lay at the distal left ventricular apex. Left ventricular end-diastolic pressure (LVEDP), left ventricular ejection fraction (LVEF), end-diastolic volume (EDV), and end-systolic volume (ESV) by cineventriculography were also evaluated. Because three patients had aortic valve replacement, we were not able to insert a catheter into the left ventricle and not able to evaluate LVEDP.

The pacemaker for CRT was the triple-output device (InSync 8040, Medtronic, Minneapolis, MN, USA) in 11 patients. In six patients, a dual-chamber pacemaker (Kappa 731, Medtronic) was implanted with a bipolar Y-adapter (5866-38M, Medtronic) for connecting the right ventricular and left ventricular leads. The left ventricular pacing lead [model 2187 ($n = 11$) or model 4023 ($n = 6$), Medtronic] was inserted by transvenous approach through the coronary sinus vein laterally ($n = 8$) or postero-laterally ($n = 7$) or antero-laterally ($n = 2$). The pacemaker device was programmed with the DDD mode of a lower rate limit at 60 bpm. The maximal tracking rate was determined by cardiopulmonary exercise testing before CRT. The atrioventricular interval was adjusted to maximize left ventricular filling time using Doppler echocardiography,[15] and no adjustment was made for the interventricular interval. We did not change these pacing modes for the chronic study. Thereafter, their hospitalization was continued for at least 1 month in order to make sure that the same medications were continued and the same daily activity was maintained for the study periods.

Clinical parameters and exercise tolerance

Clinical parameters and exercise tolerance were evaluated before and 1 month after CRT. QRS duration on standard 12-lead ECG, cardiothoracic ratio (CTR) on chest X-ray, and brain natriuretic peptide (BNP) were also obtained. A 6 min walk test was carried out and the total walking distance was determined. For quantitative evaluation for exercise tolerance, cardiopulmonary exercise testing was performed using a bicycle ergometer.[16,17] In addition, the peak oxygen uptake (peak VO_2) was calculated (Oxycon Alpha, Jaeger, Wurzburg, Germany). Because three patients had severe heart failure with NYHA functional class IV, they were not able to undergo cardiopulmonary exercise testing.

Statistical analysis

Data are presented as mean ± SD. Paired *t*-tests were performed for comparisons before and after CRT. A value of <0.05 was considered statistically significant.

Table 1 Baseline clinical characteristics

Patient number	Age (years)	Gender	Diagnosis	ECG	QRS duration (ms)	NYHA class	Medication				
							ACE-I or ARB	β-Blocker	Furosemide	Spironolacton	Digitalis
1	72	Male	DCM	CRBBB	192	IV	+	+	+	−	−
2	75	Female	DCM	RV pacing	240	III	+	−	+	−	+
3	65	Female	DCM	CRBBB	150	III	+	−	+	+	+
4	50	Female	cVHD	RV pacing	206	III	+	−	+	+	−
5	74	Male	cVHD	CLBBB	174	III	+	+	+	−	+
6	67	Male	DCM	RV pacing	219	III	+	−	+	+	+
7	68	Male	CAD	IVCD	176	III	+	+	+	+	+
8	53	Male	DCM	CLBBB	139	III	+	+	+	+	+
9	62	Male	DCM	IVCD	123	III	+	+	+	+	−
10	49	Male	DCM	IVCD	127	IV	+	−	+	−	−
11	84	Female	cASD	CLBBB	132	III	+	+	+	+	−
12	53	Female	DCM	IVCD	147	III	+	+	−	−	−
13	60	Male	CAD	IVCD	123	III	+	+	+	+	+
14	60	Male	cVHD	CLBBB	145	III	+	+	+	−	−
15	55	Male	DCM	IVCD	123	III	+	+	+	−	+
16	53	Male	DCM	IVCD	132	IV	+	+	+	−	−
17	76	Female	cVHD	RV pacing	187	III	+	−	+	−	+

DCM, dilated cardiomyopathy; cVHD, corrected valvular heart disease; CAD, coronary artery disease; cASD, corrected atrial septal defect; CRBBB, complete right bundle branch block; CLBBB, complete left bundle branch block; RV, right ventricular; IVCD, intraventricular conduction disturbance; ACE-I, angiotensin-converting enzyme-inhibitor; ARB, angiotensin receptor blocker.

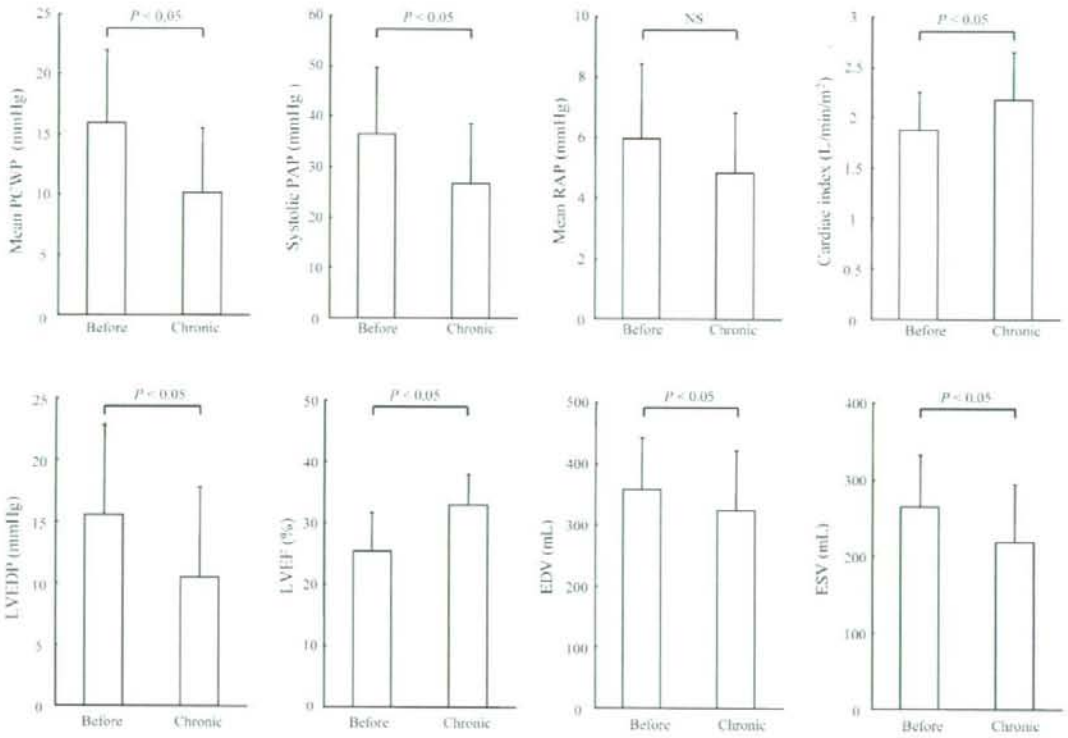

Figure 1 Effects of cardiac resynchronization therapy on chronic haemodynamics. Chronic cardiac resynchronization therapy induced a statistically significant decrease in mean pulmonary capillary wedge pressure, systolic pulmonary artery pressure, left ventricular end-diastolic pressure, end-diastolic volume, and end-systolic volume in comparison with those before cardiac resynchronization therapy. Chronic cardiac resynchronization therapy significantly increased cardiac index and left ventricular ejection fraction. However, mean right atrium pressure did not change. PCWP, pulmonary capillary wedge pressure; PAP, pulmonary artery pressure; RAP, right atrial pressure; LVEDP, left ventricular end-diastolic pressure; LVEF, left ventricular ejection fraction; EDV, end-diastolic volume; ESV, end-systolic volume.

Results

Table 1 shows the baseline clinical characteristics of enrolled patients. As shown in *Table 1*, the aetiology of heart failure was various, including dilated cardiomyopathy and corrected valvular heart disease. Two patients had coronary artery disease. Thus, the majority of enrolled patients had non-ischaemic cardiomyopathy. The aetiology of QRS prolongation was also various, including intraventricular conduction disturbance, complete left bundle branch block, complete right bundle branch block, and right ventricular pacing. The mean QRS duration before CRT was 161 ± 37 ms. Although all patients were in NYHA class III ($n = 14$) or IV ($n = 3$), they were in stable clinical condition on several kinds of medications. Because six patients did not tolerate β-blockers, they were not on them.

Haemodynamics

Chronic CRT (1 month after CRT) significantly decreased QRS duration from 161 ± 37 to 130 ± 24 ms ($P < 0.05$, $n = 17$). Chronic CRT did not change systolic blood pressure (98.2 ± 16.1 mmHg before CRT to 91.8 ± 13.8 mmHg after CRT, NS, $n = 17$) and heart rate (67.3 ± 8.9 bpm before CRT to 69.6 ± 6.0 bpm after CRT, NS, $n = 17$) at the time of cardiac catheterization. As shown in *Figure 1*, chronic CRT not only produced significant decreases in all pressure values (except right atrial pressure) but also reversed cardiac remodelling with increased LVEF and decreased EDV and ESV.

Clinical parameters and exercise tolerance

Chronic CRT significantly ($P < 0.05$ for all) improved NYHA classification, decreased CTR on chest X-ray, decreased BNP, increased 6 min walk distance, and increased peak VO_2 (*Figure 2*).

Discussion

Although the sample size is small, this is the first report which described chronic effects of CRT on invasive haemodynamics with clinical parameters as well as quantitative exercise tolerance measurements. Our study demonstrated that chronic CRT improved invasive haemodynamics (mean PCWP, systolic pulmonary artery pressure, cardiac index, LVEDP, LVEF, EDV, ESV), clinical parameters (NYHA, CTR, BNP), and exercise tolerance (6 min walk distance, peak VO_2).

Baseline characteristics and chronic effects

As apparent from the baseline values of LVEF (mean 25.4%), BNP (mean 644 pg/mL), and peak VO_2 (mean 12.8 mL/min/

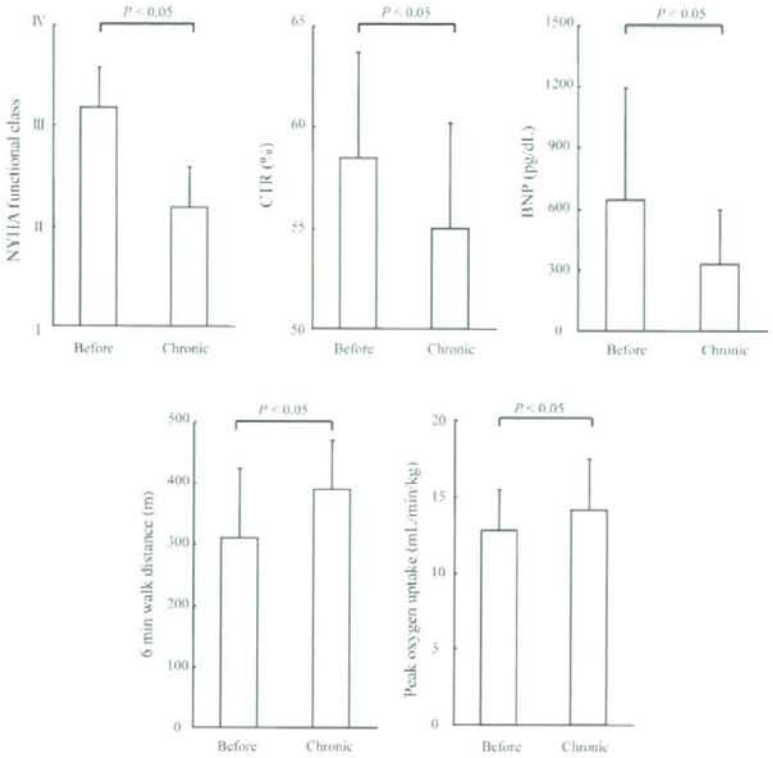

Figure 2 Effects of chronic cardiac resynchronization therapy on clinical parameters. Significant increases were observed for 6 min walk distance and peak oxygen uptake (VO_2). A significant improvement was observed for New York Heart Association (NYHA) functional class. Significant decreases were observed for cardiothoracic ratio (CTR) on chest X-ray and brain natriuretic peptide (BNP).

kg), the enrolled subjects had severe cardiac dysfunction with decreased exercise tolerance, in spite of optimal medical treatments. Accordingly, we chose CRT as the last treatment. Recently, Steendijk *et al.*[18] have published results of invasive haemodynamic effects of chronic (6 months) CRT. Our results were very similar to those of Steendijk *et al.*,[18] the mean decrease in LVEDP in their study was 5 vs. 5 mmHg in our study, the increase in cardiac output was 0.4 vs. 0.49 L/min, the increase in LVEF was 11 vs. 8%, and the decrease in EDV was 52 vs. 36 mL. Thus, our study not only confirmed the previous results by Steendijk *et al.*[18] but also suggests that chronic haemodynamic improvements and reverse cardiac remodelling occur in as much as 1 month after CRT. Although the improvement of exercise tolerance evaluated by 6 min walk distance was reported, 6 min walk test is somewhat subjective. In this study, we evaluated exercise tolerance with the very quantitative way. Peak VO_2 was significantly increased, associated with longer 6 min walk distance and improved NYHA classification status. Thus, our study confirmed the previous reports.[16,17]

Although there was no control group in our study, we do not think that the improvements reflected the natural course. As stated in the Methods section, the enrolled patients were hospitalized for at least 1 month prior to the study in order to be stable condition. We followed-up them carefully on the same daily activity and same medications in our ward. We studied them at the point when no further improvement was anticipated with optimal medical treatment.

Limitations

As stated often in the earlier discussion, the number of patients was small. We obtained invasive haemodynamics 1 month after CRT, which may have been too short in the clinical point of view. The aetiology of heart failure was heterogeneous. It is possible that chronic haemodynamic responses may differ depending on the aetiology. We studied patients with severe heart failure. It is possible that chronic haemodynamic responses may differ depending on the severity of heart failure. Finally, there was no control group.

Conclusions

Chronic CRT improved symptoms, exercise tolerance, and invasive haemodynamics associated with reversed cardiac remodelling in patients with severe heart failure and conduction delay.

Conflict of interest: none declared.

References

1. Xiao HB, Brecker SJD, Gibson DG. Effects of abnormal activation on the time course of the left ventricular pressure pulse in dilated cardiomyopathy. *Br Heart J* 1992;**68**:403–7.
2. Grines CL, Bashore TM, Boudoulas H, Olson S, Shafer P, Wooley CF. Functional abnormalities in isolated left bundle branch block. The effect of interventricular asynchrony. *Circulation* 1989;**79**:845–53.
3. Baldasseroni S, Opasich C, Gorini M, Lucci D, Marchionni N, Marini M *et al*. Left bundle-branch block is associated with increased 1-year sudden and total mortality rate in 5517 outpatients with congestive heart failure. A report from the Italian network on congestive heart failure. *Am Heart J* 2002;**143**:398–405.
4. Linde C, Braunschweig F, Gadler F, Bailleul C, Daubert JC. Long-term improvements in quality of life by biventricular pacing in patients with chronic heart failure: results from the MUltisite STImulation in Cardiomyopathy study (MUSTIC). *Am J Cardiol* 2003;**91**:1090–5.
5. Abraham WT, Fisher WG, Smith AL, Delurgio DB, Leon AR, Loh E *et al*. Cardiac resynchronization in chronic heart failure. *N Engl J Med* 2002; **346**:1845–53.
6. Cazeau S, Leclerco C, Lavergne T, Walker S, Varma C, Linde C *et al*. Effects of multisite biventricular pacing in patients with heart failure and intraventricular conduction delay. *N Engl J Med* 2001;**344**:873–80.
7. Gras D, Leclercq C, Tang AS, Bucknall C, Luttikhuis HO, Kirstein-Pedersen A. Cardiac resynchronization therapy in advanced heart failure the multicenter InSync clinical study. *Eur J Heart Failure* 2002;**4**:311–20.
8. Bradley DJ, Bradley EA, Baughman KL, Berger RD, Calkins H, Goodman SN *et al*. Cardiac resynchronization and death from progressive heart failure. A meta-analysis of randomized controlled trials. *JAMA* 2003; **289**:730–40.
9. Cleland JG, Daubert JC, Erdmann E, Freemantle N, Gras D, Kappenberger L *et al*. The effect of cardiac resynchronization on morbidity and mortality in heart failure. *N Engl J Med* 2005;**352**:1539–49.
10. Cazeau S, Alonso C, Jauvert G, Lazarus A, Ritter P. Cardiac resynchronization therapy. *Europace* 2004;**5**:S42–8.
11. Yu CM, Chau E, Sandeson JE, Fan K, Tang MO, Fung WH *et al*. Tissue Doppler echocardiographic evidence of reverse remodeling and improved synchronicity by simultaneously delaying regional contraction after biventricular pacing therapy in heart failure. *Circulation* 2002;**105**: 438–45.
12. St John Sutton MG, Plappert T, Abraham WT, Smith AL, DeLurgio DB, Leon AR *et al*. Effect of cardiac resynchronization therapy on left ventricular size and function in chronic heart failure. *Circulation* 2003;**107**: 1985–90.
13. Saxon LA, De Marco T, Schafer J, Chatterjee K, Kumar UN, Foster E. Effect of long-term biventricular stimulation for resynchronization on echocardiographic measures of remodeling. *Circulation* 2002;**105**: 1304–10.
14. Erbel R, Schweizer P, Lambertz H, Henn G, Meyer J, Krebs W *et al*. Echoventrriculography—a simultaneous analysis of two-dimensional echocardiography and cineventriculography. *Circulation* 1983;**67**: 205–15.
15. Ishikawa T, Sumita S, Kimura K, Kikuchi M, Kosuge M, Kuji N *et al*. Prediction of optimal atrioventricular delay in patients with implanted DDD pacemakers. *PACE* 1999;**22**:1365–71.
16. Varma C, Sharma S, Firoozi S, McKenna WJ, Daubert JC. Atriobiventricular pacing improves exercise capacity in patients with heart failure and intraventricular conduction delay. *J Am Coll Cardiol* 2003;**41**:582–8.
17. Auricchio A, Kloss M, Trautmann SI, Rodner S, Klein H. Exercise performance following cardiac resynchronization therapy in patients with heart failure and ventricular conduction delay. *Am J Cardiol* 2002;**89**: 198–203.
18. Steendijk P, Tulner SA, Bax JJ, Oemrawsingh PV, Bleeker GB, van Erven L *et al*. Hemodynamic effect of long-term cardiac resynchronization therapy. Analysis by pressure-volume loops. *Circulation* 2006;**113**: 1295–304.

Free Radical Research, January 2009; 43(1): 37–46

informa
healthcare

Time-dependent changes of myocardial and systemic oxidative stress are dissociated after myocardial infarction

TAKAHIRO INOUE[1], TOMOMI IDE[1], MAYUMI YAMATO[2], MASAYOSHI YOSHIDA[1], TAKAKI TSUTSUMI[1], MAKOTO ANDOU[1], HIDEO UTSUMI[3], HIROYUKI TSUTSUI[4], & KENJI SUNAGAWA[1]

[1]*Department of Cardiovascular Medicine, Graduate School of Medical Sciences,* [2]*Department of REDOX Medicinal Science,* [3]*Department of Bio-functional Science, Graduate School of Pharmaceutical Sciences, Kyushu University, Fukuoka 812-8582, Japan, and* [4]*Department of Cardiovascular Medicine, Hokkaido University Graduate School of Medicine, Sapporo 060-8638, Japan*

Accepted by Professor G. Mann

(Received 10 July 2008; revised 17 September 2008)

Abstract

Reactive oxygen species (ROS) is increased in myocardium after myocardial infarction (MI), which may play a causal role in cardiac remodelling. However, there is scant direct and longitudinal evidence that systemic oxidative stress is enhanced accompanying an increase of ROS in myocardium. The authors conducted a comprehensive investigation of ROS markers by simultaneously sampling urine, blood and myocardium and *in vivo* ESR for the heart at different stages of post-MI cardiac remodelling in mouse with permanent occlusion of left coronary artery. Systemic oxidative markers increased at early days after MI and were normalized later. In contrast, TBARS and 4-hexanoyl-Lys staining were increased in non-infarct myocardium at day 28. The enhancement of ESR signal decay of methoxycarbonyl-PROXYL measured at the chest was associated with the progression of left ventricle dilatation and dysfunction. This study provided the direct evidence that redox alteration and production of ROS occurred in myocardium during the progression of cardiac remodelling and failure; however, ROS marker levels in blood and urine do not reflect the production of ROS from failing myocardium.

Keywords: *Myocardial remodelling, oxidative stress markers, heart failure, in vivo ESR*

Abbreviations: *LV, left ventricular; MI, myocardial infarction; HF, heart failure; RAS, renin-angiotensin system; ROS, reactive oxygen species; MMP, matrix metalloproteinase; TBARS, thiobarbituric acid reactive substances; 8-OH-dG, 8-hydroxy-2′-deoxyguanosine; GPx, glutathione peroxidase; SOD, superoxide dismutase; HEL, Nε-(Hexanoyl) Lysin; ESR, electron spin resonance; FS, fractional shortening; HR, heart rate; LVEDD, left ventricular end-diastolic dimension; LVESD, left ventricular end-systolic dimension; 3-methoxycarbonyl-PROXYL, 3-methoxycarbonyl-2,2,5,5-tetramethylpyrrolidine-1-oxyl*

Introduction

Pathological left ventricular (LV) remodelling after myocardial infarction (MI) is increasingly recognized as the major cause of heart failure (HF) [1]. MI induces alterations of LV architecture with scar formation, ventricular dilatation and hypertrophy of the non-infarct myocardium [2]. In the process of remodelling, activation of various neurohumoral factors and inflammatory response, including activation of the

Correspondence: Tomomi Ide, MD, PhD, Department of Cardiovascular Medicine, Kyushu University Graduate School of Medicine, 3-1-1, Maidashi, Higashi-ku, Fukuoka 812-8582, Japan. Tel: +81-92-642-5360. Fax: +81-92-642-5374. Email: tomomi_i@cardiol.med.kyushu-u.ac.jp

ISSN 1071-5762 print/ISSN 1029-2470 online
DOI: 10.1080/10715760802534820

renin-angiotensin system (RAS), contributes to healing and scar formation in the infarct myocardium. At the end of the repairing process, cardiac hypertrophy due to haemodynamic overload is associated with hypertrophic growth of cardiomyocytes accompanying fibrosis and inappropriate interstitial collagen formation. The prognosis of HF remains poor even with wide use of RAS inhibitors and β adrenergic receptor blockers [3]. Recently, growing evidence has suggested that reactive oxygen species (ROS) are involved in the pathophysiology of myocardial remodelling and failure [4–10] and increases of ROS have been shown in various animal models of HF. We and others have demonstrated that generation of ROS is increased in post-MI myocardium in mice [9] and that treatment with antioxidants or over-expression of antioxidant enzymes prevents cardiac remodelling [11–13], resulting in improvement of survival after MI [12,13]. *In vitro* experiments demonstrated that ROS mediate hypertrophy in cardiomyocytes induced by neurohumoral factors such as angiotensin II and catecholamines, as well as cytokines including TNFα [14–17]. ROS modulate extracellular matrix function via their effects on fibroblast proliferation and collagen synthesis, involving redox-sensitive activation of matrix metalloproteinases (MMPs) [11,18,19]. Moreover, ROS alter gene expression in the case of intracellular Ca^{2+} overload, activating various proteases and promoting apoptosis in cardiomyocytes [20,21]. The above findings thus strongly suggest that redox regulation may be a potential therapeutic strategy for cardiac remodelling and HF. However, despite much discussion on the biological activities of ROS in remodelling, there is scanty clinical or animal experimental evidence for elevation of systemic oxidative biomarkers corresponding to the increase of ROS in the remodelling myocardium. We thus examined the time courses of oxidative stress in the post-MI myocardium and in systemic circulation by performing simultaneous sampling of urine, blood and myocardium during the post-MI course in a HF mouse model. Since the effects of ROS depend on a balance between the pro-oxidant molecules generated and the antioxidant reserve *in vivo*, both components should be tested to obtain better understanding of the effects of ROS on the progression of remodelling. For a comprehensive investigation of oxidative stress, we measured the byproducts of ROS represented by thiobarbituric acid reactive substances (TBARS) and 8-hydroxy-2′-deoxyguanosine (8-OH-dG), as well as the antioxidant defense capacity indicated by scavenger enzymes. Moreover, excised biological specimens only enable one to identify the target of ROS after the exposure to ROS but not to reflect the dynamic changes of redox status *in vivo* in the chronic HF model. Accordingly, we applied *in vivo* ESR to estimate redox status non-invasively in the process of remodelling using a post-MI HF model in mice.

Materials and methods

Animal model

This experiment conformed with the Guide for the Care and Use of Laboratory Animals published by the US National Institute of Health and was reviewed and approved by the Committee of the Ethics on Animal Experiment, Kyushu University Graduate School of Medical Sciences, and performed in compliance with the relevant Law (No. 105) and Notification (No. 6) of the Japanese Government.

Six week-old CD-1 male mice were purchased from Kyudo Co., Ltd. (Saga, Japan). The mice were housed in a temperature- and humidity-controlled room. MI was experimentally induced in mice by ligating the left coronary artery permanently, as previously reported [11]. The mice were assigned randomly into five groups; post-MI days 1, 4, 7, 14 and 28, and the survived mice (survived/operated: $n = 6/7$, 6/8, 10/14, 9/11, 14/21, respectively) were used in the experiments on the assigned days. Urine, blood and myocardium samples were collected from each mouse. The myocardial samples of all six mice on post-MI day 4 and six mice on post-MI day 28 were examined immunohistochemically, while the samples of the other mice were used for biochemical analysis. The data were compared with those from control mice that underwent sham operation without coronary artery ligation at day 28 ($n = 7$).

Echocardiography and haemodynamic measurements

Echocardiographic studies were performed under light anaesthesia by an intraperitoneal injection of sodium pentobarbital, with spontaneous respiration before the animal was euthanized. A 2D parasternal short-axis view of the LV was obtained by applying the transducer lightly to the mid-upper left anterior chest wall. The transducer was then gently moved cephalad or caudad and angulated until desirable images were obtained. After ensuring that the image was on axis (based on roundness of the LV cavity), 2D targeted M-mode tracings were recorded at a paper speed of 50 mm/s. Our previous study showed small intra-observer and inter-observer variabilities of our echocardiographic measurements for LV dimensions and high reproducibility of measurements made in the same animals on separate days [22]. Under the same anaesthesia with Avertin, a 1.4 Fr micromanometer-tipped catheter (Millar Instruments) was inserted into the right carotid artery and then advanced into the LV for the measurement of LV pressures for the assessment of severity of HF at day 28 after MI.

Blood sampling

Blood sample was collected with 1:500 dilution of heparin just before euthanizing each animal. Plasma was separated by centrifugation at $1000 \times g$ for 15 min at 4°C and stored at −80°C until analysis. The erythrocyte fraction was washed three times with isotonic NaCl. A stock haemolysate was prepared by the addition of the 2-mercaptoethanol-EDTA stabilizing solution. The concentrated haemolysate was diluted with 2% ethanol immediately before assay.

TBARS in plasma and 8-OH-dG in urine

To assess the level of systemic oxidative stress generated in the process of cardiac remodelling after MI, we measured TBARS in plasma and 8-OH-dG in urine. Plasma TBARS was measured by fluorometric analysis. The plasma was pre-treated with 10% phosphotungstic acid and 1/12 N sulphuric acid. The sample was mixed with a reagent to obtain a final concentration of 7.5% acetic acid, 2 mmol/L EDTA and 0.4% SDS and then reacted with 0.3% thiobarbituric acid (TBA) in a boiling water bath for 45 min. After cooling, the chromogen was extracted in n-butanol/pyridine (15:1, v/v). Fluorescence of the supernatant was measured at excitation and emission wavelengths of 510 and 550 nm, respectively, using a GENios Pro™ (Tecan Group Ltd. Durham, NC). The standard was prepared using 1,1,3,3, -tetraethoxypropane (TEP).

Urine samples were collected in individual metabolic cages (Nalgen, Rochester, NY). After overnight fasting, urine sample was collected from each mouse. Urine 8-OH-dG concentration was determined using a competitive ELISA kit (8-OH-dG check®, Japan, Institute for the Control of Aging, Nagoya, Japan). The value was corrected by urinary creatinine measured with a colorimetric assay kit (Sigma, St. Louis, MO).

TBARS in myocardial tissue

The myocardium was homogenized in 10 volumes of 50 mmol/L sodium phosphate buffer at 4°C for the assay of TBARS in myocardium. The homogenate was centrifuged at $4500 \times g$ for 15 min and the supernatant was used for the biochemical assay of TBARS as in plasma.

Antioxidant enzyme activities in myocardium

To determine the change in capacity of defense during the progression of cardiac remodelling, we measured the levels of antioxidant enzyme activities in the myocardium.

The enzymatic activities of glutathione peroxidase (GPx) and superoxide dismutase (SOD) were measured spectrophotometrically (Tecan Group Ltd., GENios). GPx activity was determined according to the method of Yamamoto and Takahashi [23] by following the oxidation of NADPH in the presence of GR (Oriental Yeast Co., Ltd. Tokyo, Japan), which catalyses the reduction of oxidized glutathione (GSSH) formed by GPx. One enzyme unit is defined as the amount of enzyme that oxidizes 1 μmol of NADPH per minute. SOD activity was examined by the cytochrome c method, in which xanthine and xanthine oxidase (Oriental Yeast Co., Ltd. Tokyo, Japan) were used as a source of superoxide. A unit was defined as the quantity of SOD required for 50% inhibition of the rate of cytochrome c reduction (Wako Pure Chemical Industries, Inc. Osaka, Japan). Protein concentration was determined by the Bradford assay.

Hexanoyl-Lysine adduct (HEL) immunostaining in myocardial tissue

Left ventricular myocardial sections obtained from mice at baseline, day 3 and 28 after MI were immunolabelled by a specific monoclonal anti-HEL antibody (Nikkenn SEIL Corp.). Paraffin-embedded tissue sections (5-μm thick) were deparaffinized with xylene, refixed in Bouin's solution for 20 min, immersed in PBS, incubated with 0.3% H_2O_2 in methanol for 30 min, followed by blocking with M.O.M. mouse IgG blocking reagent. The sections were further incubated with monoclonal anti-HEL antibody in M.O.M. Diluent. After rinsing with 10 mmol/L PBS, they were incubated with biotin-labelled goat anti-rabbit IgG anti-serum (1:100 dilution; DAKO A/S) for 60 min and then with avidin-biotin complex (1:100 dilution; Vectastain ABC kit) for 60 min. After rinsing, the sections were finally incubated with 0.02% 3,3-diaminobenzidine and 0.03% H_2O_2 in deionized water for 6–9 min. As a negative control, sections were incubated with normal rabbit serum instead of anti-HEL antibody.

In vivo *electron spin resonance study*

A spin probe, 3-methoxycarbonyl-2,2,5,5-tetramethylpyrrolidine-1-oxyl (methoxycarbonyl-PROXYL) was synthesized as described previously [24]. For the *in vivo* ESR measurements, 100 mmol/L isotonic methoxycarbonyl-PROXYL was administered (3 μl/g body weight) in mice intravenously. Then ESR spectra were taken at regular intervals using a L-band ESR spectrometer (JEOL Co. Ltd., Akishima, Japan) with a loop-gap resonator (33 mm i.d. and 30 mm in length), as reported previously [25,26]. The power of the 1.1 GHz microwave was 10 mW. The amplitude of the 100-kHz field modulation was 0.063 mT. The signal decay rates, which were used as an index of ROS generation, were determined from the semi-logarithmic plots of signal

intensity vs time after probe injection. Tiron or dimethylthiourea (DMTU) (3 μmol/mouse, dissolved in saline) was administered simultaneously with the probe to confirm the relationship between the signal decay and ROS generation.

Statistical analysis

All data are expressed as mean ± SEM. Between-group comparisons of the means were performed by one-way ANOVA followed by *t*-tests. Bonferroni's correction was done for multiple comparisons of means. A *p*-value less than 0.05 was considered to be statistically significant.

Results

Animal characteristics

The echocardiographic data of surviving mice at days 1, 4, 7, 14 and 28 after MI and control mice are shown in Table I. LV diameters were significantly greater in MI mice at day 4 and thereafter compared to sham-operated control mice. Moreover, MI mice had smaller fractional shortening and anterior wall thickness. There were no alterations in LV diameter and systolic function in sham-operated mice without coronary artery ligation up to day 28 after the operation (data not shown). At day 28, left ventricule LV end-diastolic pressure (LVEDP) was increased in MI (2.6 ± 0.7 vs 14.0 ± 2.3, $p < 0.01$) and LV weight (wt)/body wt (3.12 ± 0.11 vs 3.68 ± 0.17 mg/g, $p < 0.05$), RV wt/body wt (0.88 ± 0.06 vs 1.38 ± 0.11 mg/g, $p < 0.05$), lung wt/body wt (5.36 ± 0.13 vs 7.71 ± 0.80 mg/g, $p < 0.05$) were all increased in MI. The prevalence of pleural effusion was significantly higher in MI (0 vs 50%, $p < 0.01$).

Oxidative byproducts in plasma and urine

Plasma TBARS and urinary 8-OH-dG were significantly elevated at day 1 after MI (Figure 1), and declined to control levels at day 7 and thereafter.

Oxidative markers and antioxidant enzyme activity in myocardial tissue

We measured TBARS (an indicator of lipid peroxidation) and performed immunohistochemical staining of HEL in both infarct and non-infarct myocardial samples. In the infarct area, TBARS increased at day 1 and 7 after MI (Figure 2A). In the non-infarct area, on the contrary, TBARS level was not altered in the early days (days 1, 7 and 14) after MI but was elevated only at day 28.

In agreement with the results of myocardial TBARS, HEL-positive cardiomyocytes were located in the infarct area, whereas there was no staining in the non-infarct area at day 4. (Figure 3). HEL is a novel lipid hydroperoxide modified lysine residue, which is formed by oxidative modification by oxidized ω6 fatty acids such as linoleic acid or arachidonic acid. HEL is a useful biomarker for the initial stage of lipid peroxidation. Although positive staining lasted in the infarct area at day 28, the myocardium was mostly replaced by fibrous tissue and little living myocyte existed. In the non-infarct area, cardiomyocytes were hypertrophied and positively stained by HEL antibody. These suggest that lipid peroxidation starts at an early stage in the infarct area but at late remodelling stage in the non-infarct area. This is consistent with TBARS level in myocardium and indicated increased generation of ROS in the non-infarct area at day 28. The increase of TBARS in the non-infarct area was associated with a significant decline in SOD activity and a tendency of decrease in GPx activity at day 28 (Figure 4).

In vivo *ESR in the heart*

Since TBARS is known to be a non-specific assay to measure lipid peroxidation from biological fluids and tissues and many other substances besides reactive aldehydes react with TBA, we used *in vivo* ESR to determine whether the level of ROS increased in the heart in the remodelling process. Methoxycarbonyl-PROXYL, a stable membrane-permeable nitroxyl radical, is converted into its non-magnetic products, such as its hydroxylamine, immediately after the

Table I. Echocardiographic data.

		Time after MI (days)				
	Control	1	4	7	14	28
n	7	6	6	10	9	8
Heart rate (bpm)	524 ± 22	564 ± 25	552 ± 16	568 ± 23	551 ± 28	589 ± 43
LVEDD (mm)	4.0 ± 0.2	4.5 ± 0.2	5.0 ± 0.2**	5.1 ± 0.2**	5.4 ± 0.1**	5.6 ± 0.2**
LVESD (mm)	2.3 ± 0.2	3.6 ± 0.2**	3.9 ± 0.2**	3.9 ± 0.1**	4.2 ± 0.1**	4.4 ± 0.1**
Fractional shortening (%)	37.6 ± 1.6	21.1 ± 1.6**	22.2 ± 1.6**	23.2 ± 1.6**	20.7 ± 1.0**	21.0 ± 2.7**
Infarct wall thickness (mm)	0.83 ± 0.03	0.60 ± 0.05**	0.61 ± 0.03**	0.44 ± 0.02**	0.44 ± 0.06**	0.30 ± 0.08**
Non-infarct wall thickness (mm)	0.84 ± 0.04	0.80 ± 0.05	1.00 ± 0.02	1.13 ± 0.07*	1.30 ± 0.05**	1.25 ± 0.18**

Control, sham-operated mice; LV, left ventiruclar; EDD, end-diastolic dimension; ESD, end-systolic dimension.
Values are means ± SEM. * $p < 0.05$, ** $p < 0.01$ vs controls.

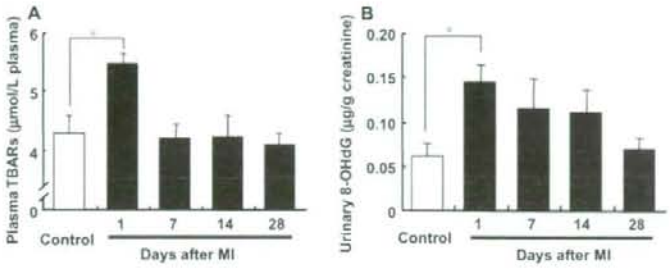

Figure 1. Time-dependent changes of plasma TBARs (A) and urinary 8-OHdG (B) in sham-operated control mice ($n=7$) and mice on day 1 ($n=6$), day 7 ($n=10$), day 14 ($n=9$) and day 28 ($n=8$) after MI. Values are means ± SEM. * $p<0.05$, ** $p<0.01$ compared with sham-operated control.

reaction with hydroxy radicals or other reductants. To determine the level of ROS or redox status by *in vivo* ESR measurements, we used methoxycarbonyl-PROXYL as a spin probe which was observed as three sharp lines by ESR spectroscopy (Figure 5A).

We applied signal decay of methoxycarbonyl-PROXYL to *in vivo* ESR to measure ROS generation non-invasively in the failing heart in mice after MI. When the ESR spectrum was measured at the chest level, the signal decay rate was greater in MI mice than sham-operated mice (Figure 5B). The increase of the signal decay observed in MI was suppressed by a simultaneous injection of antioxidants, Tiron or DMTU (Figure 5C and D), indicating the enhancement of free radical reactions at the chest in MI mice. To confirm that the enhancement of signal decay is localized at the chest and does not reflect the increase of systemic free radical generation, the same ESR measurement was repeated at the other parts of the body, head and abdomen from the same animals. ESR signal decay was similar between the two groups when the spectrum was detected at the head and abdominal levels (Figure 5E and F).

Redox alteration during the process of remodelling after MI

Using this *in vivo* ESR technique, we measured free radical production during the time course of remodelling after MI in mice. Radical generation was increased gradually in 4 weeks after MI, which was in parallel to the increase of LVEDD and LVESD and the decrease of EF assessed by echocardiography (Figure 6).

Discussion

In the post-MI myocardium, early remodelling occurs accompanied by infarct expansion, regional dilatation and thinning of the infarct zone and is followed by further deterioration in cardiac performance and increased neurohormonal activation in late remodelling. ROS play an important role in the progression of remodelling in the post-MI myocardium. However, phase-dependent alteration of ROS production in the post-MI myocardium has not been discussed. Moreover, despite a lack of evidence, it is widely misconstrued that an increase of local ROS production is reflected by increases of systemic ROS markers. The present study demonstrates that systemic elevations of ROS markers occur only at the earlier phase after MI. On the contrary, the generation of ROS in non-infarct myocardium is increased from the late phase.

Roles of ROS in the progression of cardiac remodelling

ROS potentially cause cellular damage and dysfunction. Whether the effects of ROS are beneficial or

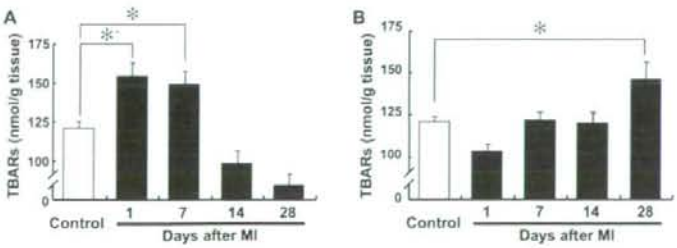

Figure 2. Time-dependent changes of TBARs in infarct (A) and in non-infarct (B) myocardium in sham-operated control ($n=7$) and on day 1 ($n=6$), day 7 ($n=10$), day 14 ($n=9$) and day 28 ($n=8$) after MI. Values are means ± SEM. * $p<0.05$ compared with sham-operated control.

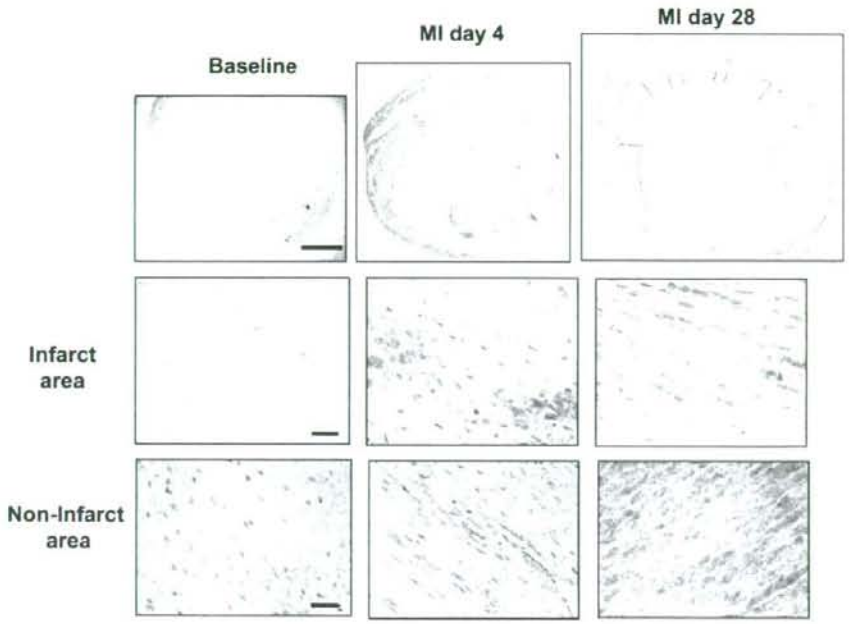

Figure 3. Immunohistochemical detection of HEL moieties in the remodelling process in whole LV, infarct myocardium and non-infarct myocardium, during acute-phase (day 4) and late-phase (day 28) after MI. Scale bar; 1 mm (top) and 10 μm (infarct area and non-infarct area).

harmful depends on the site of action, the source, the amount of ROS generation and the resulting redox balance. Several groups reported that ROS are increased in congestive HF patients [27,28] and accumulating evidence from animal studies revealed that increased ROS play a pivotal role in the pathogenesis and progression of HF [4,9,29–33]. However, whether systemic ROS markers are useful for determining the redox state of the failing heart remains unknown. Li et al. [34] used LC/MS/MS to analyse F_2-isoprostanes in urine from HF patients. They found that only a few peaks were increased, but the most abundant isomer 5-epi-8,12-iso-iP$F_{2\alpha}$-VI was comparable to control subjects. Other clinical studies examined ROS in serum or urine in HF patients by measuring redox markers and reported that ROS are elevated in functionally very poor, NYHA class III or class IV patients. At the time of acute deterioration of HF or sudden onset of cardiac ischemia, patients often have congestion or elevation of LV end diastolic pressure. In such conditions, the immune system, neurohormonal factors such as TNFα and other cytokines are activated with concurrent activation of sympathetic nerve, all of which cause endothelial damage and other organ disorders [35]. In fact, acute MI is associated with a marked increase of inflammatory cells. Previous reports have demonstrated that inflammatory responses and neurohormonal factors cause the generation of oxidative stress not only from the myocardium but also from the vasculature [36–40]. These observations are consistent with our result showing that alteration of systemic ROS markers may not always reflect ROS generation in the myocardium.

Redox status estimated by in vivo ESR

ESR spectroscopy is a useful method to estimate redox status in living animals. In this study, we demonstrated using *in vivo* ESR spectroscopy that increased generation of free radicals in the heart correlated with dilatation of LV and decrease in EF, both of which are indices of the myocardial remodelling process after MI.

There are several advantages to determine ROS generation by *in vivo* ESR spectroscopy. First, the method allows non-invasive assessment of ROS generation in an *in vivo* setting. Secondly, *in vivo* ESR can be repeated in the same animal at different time points, indicating that the ESR technique has the potential to be used as a diagnostic tool in the future. Thirdly, this ESR technique can estimate and quantify the 'net' redox state. Antioxidant enzymes and reductants (such as glutathione) in the ROS generating system together determine the total redox status in biological systems, which may change dynamically and acutely in the heart after MI. Byproducts of free oxygen radicals such as lipid